ORIGINAL ARTICLE

Synthesis and investigation of thermal properties of vanadyl complexes with azo-containing Schiff-base dyes

Abbas Ali Salih Al-Hamdani [a,*], **Abdel Majid Balkhi** [a], **A. Falah** [a], **Shayma A. Shaker** [b,*]

[a] Department of Chemistry, Faculty of Science, University of Damascus, Syria
[b] Department of Petrochemical Engineering, Technical College of Engineering, Duhok Polytechnic University, Duhok, Kurdistan Region, Iraq

Abstract Azo-Schiff base compounds (L_1 and L_2) have been synthesized from the reaction of m-hydroxy benzoic acid with 1,5-dimethyl-3-[2-(5-methyl-1H-indol-3-yl)-ethylimino]-2-phenyl-2,3-dihydro-1H-pyrazol-4-ylamine and with 3-[2-(1H-indol-3-yl)-ethylimino]-1,5-dimethyl-2-phenyl-2,3-dihydro-1H-pyrazol-4-ylamine. The free ligands and their complexes were characterized based on elemental analysis, determination of metal, molar conductivity, (^{1}H, ^{13}C) NMR, UV–vis, FT-IR, mass spectra and thermal analysis (TGA). The molar conductance data revealed that all the complexes are non-electrolytes. The study of complex formation via molar ratio in DMF solution has been investigated and results were consistent to those found in the solid complexes with a ratio of (M:L) as (1:1). Moreover, the thermodynamic activation parameters, such as ΔE^*, ΔH^*, ΔS^*, ΔG^* and K are calculated from the TGA curves using Coats–Redfern method. Hyper Chem-6 program has been used to predict the structural geometries of compounds in gas phase. The heat of formation ($\Delta H_f°$) and binding energy (ΔE_b) at 298 K for the free ligands and their vanadyl complexes were calculated by PM3 method. The synthesized ligands and their metal complexes were screened for their biological activity against bacterial species, two Gram positive bacteria (*Bacillus subtilis* and *Staphylococcus aureus*) and two Gram negative bacteria (*Escherichia coli* and *Pseudomonas aeruginosa*).

* Corresponding authors.
  E-mail addresses: Abbas_alhamadani@yahoo.co.uk (A.A.S. Al-Hamdani), drshaimaa611@yahoo.com (S.A. Shaker).
Peer review under responsibility of King Saud University.

1. Introduction

The Tryptamine class of chemicals includes naturally occurring, synthetic, and semi-synthetic drugs built on the base skeleton "Tryptamine". The important structural distinction of the tryptamine class of chemicals is its approximation to the

neurotransmitter serotonin. These drugs are commonly referred to as hallucinogens. Tryptamine type ligands, one of the oldest classes of ligands in coordination chemistry have been used extensively on complex transition and main group metals (Cambel and Nguyen, 2001). Schiff base complexes containing different metal ions such as Ni and Cu have been studied in detail for their various crystallographic features, structure–redox relationships and enzymatic reactions, mesogenic characteristics and catalysis properties (Aiello et al., 1997; Klement et al., 1999; Santos et al., 2000; Stemmler and Burrows, 1999). Transition metal complexes of Schiff bases are of paramount scientific interest, due to their multiple uses as biomimetic systems of enzymes involved in the transport, storage and activation of di oxygen (Bryliakov and Talsi, 2004; Dyers et al., 2006; Pui and Pierre, 2007; Ueno et al., 2006; Vigato and Tamburini, 2004). CuN_2O_2 coordination is very common in copper chemistry and the redox behavior of a wide series of mononuclear copper(II) Schiff base complexes was reviewed some years ago in relation to their structural changes (Bernal, 1990). Azo groups are relatively robust and chemically stable. Therefore, they prompted extensive studies of azo benzene based structures as dyes and colorants. Furthermore, the light-induced interconversion allows systems incorporating azo group to be used as photo switches, effecting rapid and reversible control over a variety of chemical, mechanical, electronic and optical properties. Because of the good thermal stability of azo compounds, one of the most important applications of azo compounds is in the optical data storage (El Halabieh et al., 2004; Nishihara, 2004). In this work a new efficient route for the synthesis of Azo-Schiff base ligands and their metal complexes has been studied. The thermal decomposition of their complexes is also used to infer the structure and different thermodynamic activation parameters are calculated. The biological activity of these ligands and their vanadyl complexes are evaluated. Hyper Chem-6 program has been used to predict the structural geometries of compounds in the gas phase.

2. Experimental

2.1. Materials and measurements

All reagents were commercially available and used without further purification. Solvents were distilled from appropriate drying agents immediately prior to use.

Elemental analyses (C, H and N) were performed using a Perkin-Elmer CHN 2400 elemental analyzer. The content of metal ions were calculated gravimetrically as metal oxides. Molar conductance measurements of the ligand and its complexes with 10^{-3} mol/l in DMSO were carried out using Jenway 4010 conductivity meter. Magnetic measurements were carried out on a Sherwood Scientific magnetic balance using the Gouy method. Electron impact (70 eV) mass spectra were recorded on a Finnegan-MAT model 8430 GC–MS-DS spectrometer. The UV vis spectra were obtained in DMF solution (10^{-3} M) for the ligands and their vanadyl complexes with a Jenway 6405 spectrophotometer using 1 cm quartz cell, in the range 200–900 nm. IR spectra (4000–400 cm^{-1}) were recorded as KBr pellets on a Bruker FT-IR spectrophotometer.

(^{1}H, ^{13}C) NMR spectra were acquired in DMSO-d_6 solution using a Bruker AMX400 MHz spectrometer with tetramethylsilane (TMS) as an internal standard for ^{1}H NMR analysis and thermal analysis studies of the ligand and complexes were performed on a Perkin-Elmer Pyris Diamond DTA/TG thermal system under nitrogen atmosphere at a heating rate of 10 °C/min from 25–700 °C.

2.2. Synthesis of the compound 1,5-dimethyl-3-[2-(5-methyl-1H-indol-3-yl)-ethylimino]-2-phenyl-2,3-dihydro-1H-pyrazol-4-ylamine (A)

An ethanolic solution (15 ml) of 5-methyltryptamine hydrochloride (1.036 g, 0.00492 mol) was added to a mixture containing an ethanolic solution (25 ml) of 4-amino-1,5-dimethyl-2-phanyl-3-pyrazol-5-one (1 g, 0.00492 mol). The mixture was heated in a water bath at 40–50 °C for 14 h in the presence of K_2CO_3 after the addition of excess of ethanol (50 ml). The resulting mixture was refluxed under N_2, a white solid was formed and then recrystallized from a mixture of water/ethanol (1:1). The product was dried over anhydrous $CaCl_2$ in vacuum. Yield: 53.76% (0.95 g), mp 177 °C. ^{1}H NMR (DMSO-d_6, ppm): δ 1.89 (s, =CCH$_3$), 2.10 (s, arom-CH$_3$), 3.43 (s, NCH$_3$), 3.30 (t, NCH$_2$), 2.74 (t, CCH$_2$), 7.64–8.08 (m, arom), 12.11 (s, NH), 4.10 (s, NH$_2$). ^{13}C NMR (100.622 MHz, DMSO-d_6): δ 16.39 (C$_{20}$), 18.87 (C$_3$), 38.79 (C$_{13}$), 45.6 (C$_{12}$), 58 (C$_1$), 98 (C$_{17}$), 100 (C$_{7,11,14}$), 110 (C$_{18}$), 111 (C$_{15,21}$), 118 (C$_4$), 123.77 (C$_9$), 127 (C$_{22}$), 129 (C$_{19}$), 130 (C$_{8,10}$), 140 (C$_6$), 146 (C$_2$), 151 (C$_5$), (MS) m/z 360, 164, 201.

2.3. Synthesis of 3-[2-(1H-indol-3-yl)-ethylimino]-1,5-dimethyl-2-phenyl-2,3-dihydro-1H-pyrazol-4-ylamine (B)

An ethanolic solution (15 ml) of tryptamine hydrochloride (0.967 g, 0.00492 mol) was added to a mixture containing an ethanolic solution (25 ml) of 4-amino-1,5-dimethyl-2-phanyl-3-pyrazol-5-one (1 g, 0.00492 mol). The reaction mixture was heated in a water bath at 40–50 °C for 14 h in the presence of K_2CO_3 after the addition of excess of ethanol (50 ml). The resulting mixture was refluxed under N_2, a brown light solid was formed, and then recrystallized from a mixture of water/ethanol (1:1). The product was dried over anhydrous $CaCl_2$ in vacuum. Yield: 53.59% (0.91 g), mp 144 °C. ^{1}H NMR (DMSO-d_6, ppm): δ 1.71 (s, =CCH$_3$), 2.99 (s, NCH$_3$), 2.17 (t, NCH$_2$), 1.92 (t, CCH$_2$), 7.64–8.00 (m, arom), 10.99 (s, NH), 5.99 (s, NH$_2$). ^{13}C NMR (100.622 MHz, DMSO-d_6): δ_C (100.622 MHz, DMSO-d_6): 15.6 (C$_{20}$), 35.1 (C$_3$), 40.6 (C$_{13}$), 58 (C$_{12}$), 118 (C$_1$), 121 (C$_{7,11,14}$), 128 (C$_{9,18}$), 133 (C$_{15,16}$), 136 (C$_4$), 140 (C$_{17}$), 147 (C$_{8,10,19}$), 157 (C$_6$), 167 (C$_2$), 178 (C$_5$).

2.4. Synthesis of ligand (L$_1$) 2-[1,5-dimethyl-3-[2-(5-methyl-1H-indol-3-yl)-ethylimino]-2-phenyl-2,3-dihydro-1H-pyrazol-4-ylazo]-5-hydroxy-benzoic acid

A mixture solution from H_2SO_4 (18 M, 2 ml), ethanol (10 ml) and distilled water (10 ml), were charged with (A) (0.5 g, 1.39 mmol). An aqueous solution (2 ml) of NaNO$_2$ (0.0144 g, 1 mmol) was added to the mixture in drops while maintaining
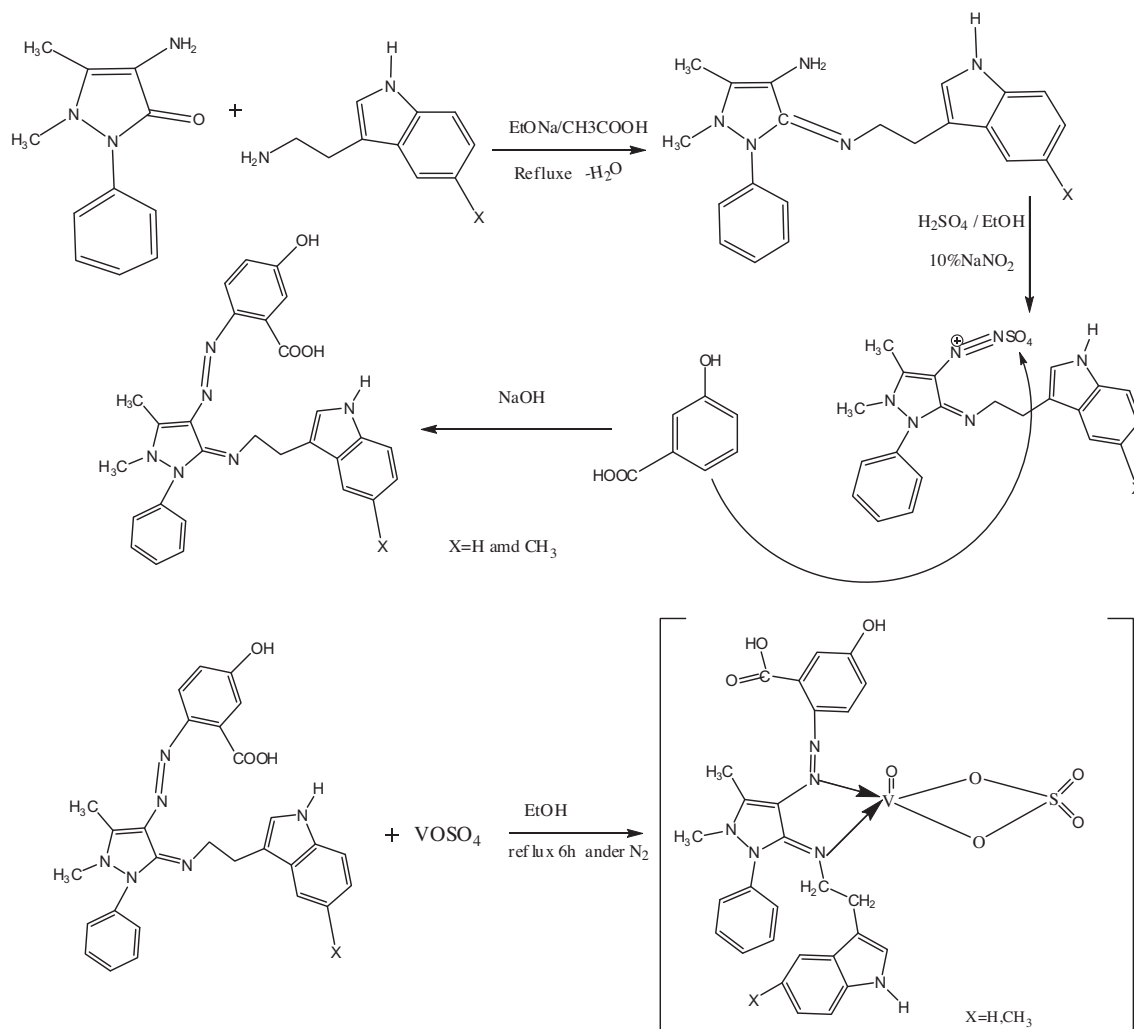
Scheme 1 Syntheses of vanadyl complexes.

the temperature between 0 and 5 °C. After that the diazonium chloride was added, respectively, with constant stirring to cold ethanolic solution of *m*-hydroxy benzoic acid (0.192 g, 1.39 mol), and then a solution of 1 M NaOH (25 ml) was added to the dark colored mixture. The mixture was stirred for 1 h at 0 °C and acidified with 1 mL of conc. HCl. The brown product formed was suction filtered and recrystallized from ethanol/water (1:1) and dried as shown in Scheme 1. Yield: 62.2% (0.44 g), mp > 390 °C.

^{1}H NMR (DMSO-d_6, ppm): 1.89 (s, C–CH$_3$), 2.10 (s, arom-CH$_3$), 3.43 (s, NCH$_3$), 3.30 (t, NCH$_2$), 2.74 (t, CCH$_2$), 4.49 (s, O–H phenol), 7 (d, C$_{25}$-H), 7.23 (s, C$_{15}$-H), 7.36 (m, C$_{7,11}$-H), 7.44 (m, C$_{9,18,21}$-H), 7.85 (d, C$_{24}$-H), 7.90 (m, C$_{8,10}$-H), 8.08 (d, C$_{17}$-H), 12.11 (d, N–H), 13 (s, O–H carboxylic). ^{13}C NMR (100.622 MHz, DMSO-d_6) δ 16.39 (C$_{20}$), 18.87 (C$_3$), 38.79 (C$_{13}$), 45.6 (C$_{12}$), 58 (C$_1$), 98 (C$_{17}$), 100 (C$_{7,11,14}$), 106 (C$_{25}$), 110 (C$_{18}$), 111 (C$_{23}$), 111 (C$_{15,21}$), 118 (C$_4$), 123.77 (C$_9$), 127 (C$_{24}$), 128 (C$_{26}$), 129 (C$_{19}$), 130 (C$_{8,10}$), 140 (C$_6$), 144 (C$_{27}$), 146 (C$_{22}$), 146 (C$_2$), 151 (C$_5$), 152 (C$_{29}$), 182 (C$_{28}$), (MS) *m/z* 508 (C$_{29}$H$_{28}$N$_6$O$_3$), 345 (C$_{18}$H$_{15}$N$_5$O$_3$)$^{2-}$, 159 (C$_{11}$H$_{13}$N).

2.5. Synthesis of ligand (L$_2$) 5-hydroxy-2-{3-[2-(1H-indol-3-yl)-ethylimin-1,5-dimethyl-2-phenyl-2,3-dihydro-1H-pyrazol}-benzoic acid

A mixture solution from H$_2$SO$_4$ (18 M, 2 ml), ethanol (10 ml) and distilled water (10 ml), was charged with (B) (0.5 g, 0.0014 mol). An aqueous solution (2 ml) of NaNO$_2$ (0.0144 g, 0.001 mol) was added to the mixture in drops while maintaining the temperature between 0 and 5 °C. After that the diazonium sulfate was added, respectively, with constant stirring to a cold ethanolic solution of *m*-hydroxy benzoic acid (0.192 g, 0.0014 mol), and then a solution of 1 M NaOH (25 ml) was added to the dark colored mixture. The mixture was stirred for 1 h at 0 °C and acidified with 1 mL of conc. HCl. The red light product formed was suction filtered and recrystallized from ethanol/water (1:1) Scheme 1. Yield: 64.08% (0.43 g), mp > 390 °C. ^{1}H NMR (DMSO-d_6, ppm): 1.70 (s, C–CH$_3$), 2.10 (s, NCH$_3$), 3.30 (t, NCH$_2$), 2.74 (t, CCH$_2$), 4.49 (s, O–H phenol), 7 (d, C$_{25}$-H), 7.23 (s, C$_{15}$-H), 7.36 (m, C$_{7,11}$-H), 7.44 (m, C$_{9,18,21}$-H), 7.85 (d, C$_{24}$-H), 7.90 (m, C$_{8,10}$-H), 8.08 (d, C$_{17}$-H), 10.99 (d, N–H), 12.11 (s, O–H

carboxylic). ^{13}C NMR (100.622 MHz, DMSO-d_6) δ 16.39 (C_{20}), 18.87 (C_3), 38.79 (C_{13}), 45.6 (C_{12}), 58 (C_1), 98 (C_{17}), 100 ($C_{7,11,14}$), 106 (C_{25}), 110 (C_{18}), 111 (C_{23}), 111 ($C_{15,21}$), 118 (C_4), 123.77 (C_9), 127 (C_{24}), 128 (C_{26}), 129 (C_{19}), 130 ($C_{8,10}$), 140 (C_6), 144 (C_{27}),146 (C_{22}), 146 (C_2), 151 (C_5), 152 (C_{29}), 182 (C_{28}).

2.6. Syntheses of vanadyl complexes

Vanadyl complexes were prepared in a similar manner using the method described by Nejati and Rezvani elsewhere as shown in Scheme 1. Thus, a solution of 4 mmol of VOSO$_4$ H$_2$O in 10 ml of ethanol was added to an ethanol chloroform (1:1 v/v) solution containing 8 mmol of ligand and was refluxed for 6 h. The obtained solution was left at room temperature. Vanadyl complexes were obtained as violet microcrystals with L$_1$, and Vanadyl complexes were obtained as green dark microcrystals. The microcrystals were filtered off, washed with absolute ethanol and then recrystallized from ethanol/chloroform (1:3 v/v). VOL$_1$, violet, yield 66%. VOL$_2$ green dark, yield 66%.

2.7. Microbiological investigations

For these investigations the filter paper disc method was applied according to Gupta et al. (1995). The investigated isolates of bacteria were seeded in tubes with nutrient broth (NB). The seeded NB (1 cm^3) was homogenized in tubes with 9 cm^3 of melted (45 °C) nutrient agar (NA). The homogeneous suspensions were poured into Petri dishes. The discs of filter paper (diameter 4 mm) were ranged on the cool medium. After cooling on the formed solid medium, 2×10^{-5} dm^3 of the investigated compounds were applied using a micropipette. After incubation for 24 h in a thermostat at 25–27 °C, the inhibition (sterile) zone diameters (including disc) were measured and expressed in mm. An inhibition zone diameter over 7 mm indicates that the tested compound is active against the bacteria under investigation. The antibacterial activities of the investigated compounds were tested against Escherichia coli and Pseudomonas aeruginosa for Gram negative and Bacillus subtilis and Staphylococcus aureus for Gram positive. The concentration of each solution was 1.0×10^{-3} mol dm^3, commercial DMSO was employed to dissolve the tested samples.

2.8. Programs used in theoretical calculation

Hyper Chem-6 program is a sophisticated molecular modeler, editor and powerful computational package, that is known for its quality, flexibility and ease of use. It is also uniting 3D visualization and animation with quantum chemical calculations, molecular mechanics and dynamics (Dorestt, 1996). In the present work, parameterization method 3(PM3) was used for

Table 1 Elemental analysis and physical data of L$_1$ and L$_2$ ligands and their vanadyl complexes.

Compound	Molecular weight	Elemental analysis Cal (Found) %					μ_{eff} B.M	Molar conductivity Ohm^{-1} cm^2 mol^{-1}
		C	H	N	M	S		
B	345.20	(73.02)	(6.71)	(20.27)	–	–	–	–
C$_{21}$H$_{23}$N$_5$		74.22	6.76	22.03				
L$_2$	494.54	(68.00)	(5.30)	(16.99)	–	–	–	–
C$_{28}$H$_{26}$N$_6$O$_3$		69.98	5.55	17.22				
A	360.20	73.51	7.01	19.48	–	–	–	–
C$_{22}$H$_{25}$N$_5$		(75.55)	(6.87)	(21.23)				
L$_1$	508.57	(68.49)	(5.55)	(16.52)	–	–	–	–
C$_{29}$H$_{28}$N$_6$O$_3$		67.76	5.83	16.56				
[VOL$_1$SO$_4$]	671.58	(51.86)	(4.20)	(12.51)	(7.59)	(4.77)	1.65	23
C$_{29}$H$_{28}$N$_6$O$_8$SV		50.43	4.01	13.12	8.15	4.12		
[VOL$_3$SO$_4$]	657.55	(51.14)	(3.99)	(12.78)	(7.75)	(4.88)	1.66	19
C$_{28}$H$_{26}$N$_6$O$_8$SV		51.09	4.09	13.02	6.77	4.31		

Table 2 Infrared data of ligands and their metal complexes (cm^{-1}).

Compound	v(OH)$_{carbox}$	v(OH)$_{ph}$ v(OH)$_{ph}$	v(NH)	v(C=O) v(C=N)	v(N=N) v(C–N=N–C)	v(M–N) v(M–O)	v(COO)as v(COO)s	Additional bands
A			3271	– 1641				asv(NH) = 3485 sv(NH) = 3305
L$_1$	3429	3699 1288	3234	1728 1692	1444 1124	–	1601 1342	–
B			3213	– 1662				asv(NH) = 3433 sv(NH) = 3329
L$_2$	3429	3692 1288	3234	1738 1699	1444 1124	–		
[VOL$_1$SO$_4$]	3422	3692 1281	3234	1727 1680	1454 1124	537	1586	v(V=O) = 924 v(SO$_4$) = 937
[VOL$_2$SO$_4$]	3423	3695 1288	3234	1724 1677	1450 1120	550 443	1600 1344	v(V=O) = 923 v(SO$_4$) = 938

Table 3 Thermal data of L_1, L_2 ligands and complexes.

Compound	TG range (°C)	DTG$_{max}$ (°C)	%Estimated (calculated)		Assignment
			Mass loss	Total mass loss	
L_1	158–348	290.36	82.648 (82.085)	101.131	$C_{23}H_{23}N_5O_3$
	348–598	513.87	18.483 (17.914)	(99.999)	$C_6H_5N^-$
L_2	153–355	289.45	70.890 (69.642)	102.231	$C_{21}H_{20}N_4O$
	355–596	528.12	31.341 (30.357)	(99.999)	$C_7H_6N_2O_2$
[VOL$_1$SO$_4$]	30–415	313.97	42.814 (42.22)	91.392	$C_{17}H_{17}NO_3$
	415–600	483.47	48.578 (48.786)	(91.006)	$C_{12}H_{17}N_5O_4S$
			8.608 (9.976)		VO
[VOL$_2$SO$_4$]	410–30	310.97	42.814 (42.22)	83.6	$C_{17}H_{17}NO_3$
	600–410	778.47	40.786 (40.225)	(82.445)	$C_{12}H_{17}N_5O_4S$
			16.4 (17.555))		VO_3S

Table 4 Thermodynamic data of the thermal decomposition of L_1 and L_2 ligands and their VO(VI) complexes.

Sam (step)	T range (°C)	n	R^2	T_{max} (K)	Ea (kJ mol^{-1})	ΔH^* (kJ mol^{-1})	A (sec$^{-1} \times 10^7$)	ΔS^* (J mol^{-1} K^{-1})	ΔG^* (kJ mol^{-1})	$K \times 10^{-7}$
L_1 (1)	158–348	1	0.99	563.51	7.6669	2.982	425.5	−104.171	61.983	1.7958
L_1 (2)	348–598	1	0.99	786.85	12.2404	5.6986	830.9	−101.378	85.467	2.1189
L_2 (1)	153–355	1	0.997	562.6	9.624628	9.15717	3.955	−104.76	68.095	4.75867
L_2 (2)	355–596	1	0.998	801.27	10.988793	4.327	11.226	−95.561	80.897	53.23
VOL$_{1=1}$	30–415	0.9	0.98	587.12	7.81693	2.935	477.07	−103.561	63.738	21.336
VOL$_{1=2}$	415–600	0.9	0.99	756.62	13.19058	4.4058	7259.5	−85.8097	95.074	199.436
VOL$_{2=1}$	30–410	0.9	0.987	584.12	6.775224	1.91885	5.796	−101.9003	61.4408	0.320245
VOL$_{2=2}$	410–600	0.9	0.998	1051.62	12.10735	3.3725	2.76287	−112.95058	122.1535	8.55723

the calculation of heat of formation and binding energy for all metal complexes. PM3 is more popular than other semi-empirical methods due to the availability of algorithms and it is more accurate than other methods (Foresman and Frisch, 1996). PM3/TM is an extension of the PM3 method to include orbitals with transition metals. It is parameterized primarily for organic molecules and selected transition metals.

3. Results and discussions

Bidentate complexes were obtained upon reaction between vanadyl ion and (L_1 and L_2) ligands at 1:1 M ratio. The synthesized azo-Schiff base ligands and their complexes are very stable at room temperature in the solid state. The ligands and their vanadyl complexes are generally soluble in hot DMF and DMSO. The yields, melting/decomposition points, elemental analyses, magnetic measurements, and molar conductance of (L_1 and L_2) and its vanadyl complexes are presented in Table 1. The analytical data are in good agreement with the proposed stoichiometry of the complexes. The metal-to-ligand ratio of complexes was found to be 1:1. The ligand decomposed at temperatures higher than 250 °C, while all complexes decomposed at temperatures higher than 300 °C. The ligands and their vanadyl complexes have dye character due to the high molar extinction constant. Elemental analyses are in good agreement with the proposed formula.

3.1. Molar conductivity of metal chelates

The vanadyl complexes discussed herein were dissolved in DMF and the molar conductivities of their 10^{-3} M solutions

at room temperature were measured to establish the charge of the metal complexes. The range of conductance values listed in Table 1 indicates that all the metal complexes have non-electrolyte nature (Golcu et al., 2005). These results are confirmed by the elemental analysis data because the SO_4^{2-} ions are not precipitated. This test matches well with C, H and N data. Thus, the ligands and their complexes did not have electrolytic properties. This fact elucidated that the SO_4^{2-} ions are absent. In addition, the molar conductance values indicate that the anions may be absent or exhibit inside the coordination sphere, the sulfate ion was detected inside the coordination sphere of the complex by degradation of the complexes.

3.2. UV–vis spectra and magnetic moments

The UV–vis spectra of the ligands and their vanadyl complexes are recorded in DMF solution in the wavelength range of 200–900 nm. The electronic spectra of the free ligands (L_1 and L_2) show electronic transitions $\pi\rightarrow\pi^*$ and $n\rightarrow\pi^*$ at (275 and

Table 5 Conformation energies in (kJ mol^{-1}) for the starting material (A) and ligand.

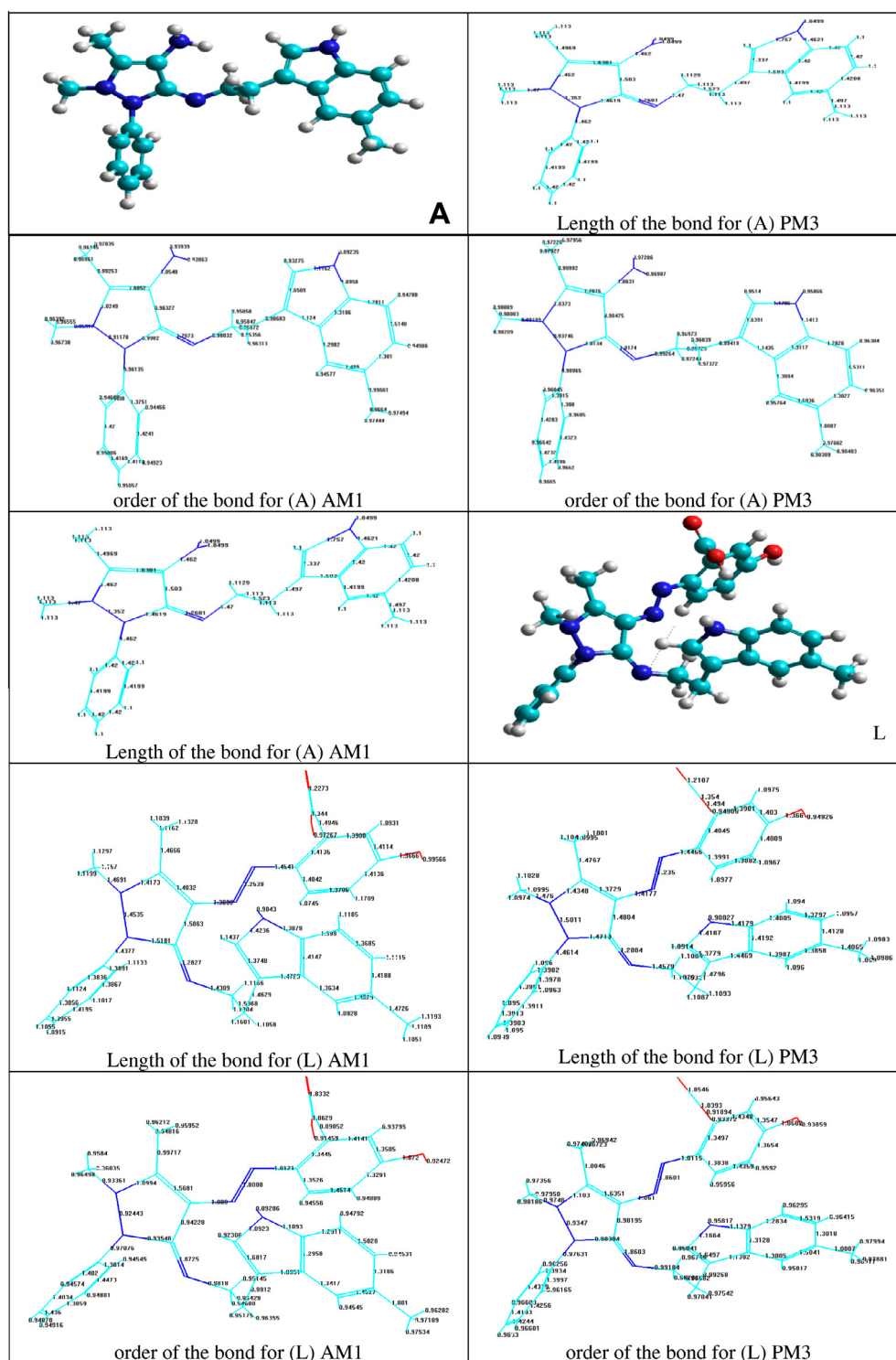| Conformation	$\Delta H_f°$	ΔE_b
A	143.0217934	−5484.108206
L_1	44.0793240	−7227.2636760
B	173.1846562	−5235.821014
L_2	101.3406824	−6894.9083176
[VOL$_1$ SO$_4$]	−45.7689019	−5890.2587901
[VOL$_2$ SO$_4$]	AMBER: $\Delta Hf° = \Delta E_b$ = −5991.2587901	

Figure 1 Conformational structure of (A and B), ligands and their complexes.

285) nm and (300 and 302) nm, respectively. The electronic spectrum of the VO(VI) complexes, exhibits intense bands at (290 and 290 nm), (34482 and 34482 cm^{-1}), (ε = 1200 and 2550 L mol^{-1} cm^{-1}) assignable to the ($\pi \rightarrow \pi^*$), respectively. Thus, the spectra of complexes exhibited bands in the visible region at (589 and 590 nm), (16977 and 16949 cm^{-1}), (ε = 680 and 520 L mol^{-1} cm^{-1}) assignable to the ($^2B_{2}g \rightarrow$ $^2B_{1}g$ π^*), respectively, and the (795 and 790 nm), (12578 and 12658 cm^{-1}), (ε = 600 and 500 L mol^{-1} cm^{-1}) assignable to the ($^2B_{2}g \rightarrow$ ^2Eg π^*), respectively, the transition, indicating a Square pyramidal geometry for this complexes. The magnetic moments of 1.65 and 1.66 BM, respectively, are a further indication of the Square pyramidal geometry (Lever, 1968a,b; Shayma et al., 2010).
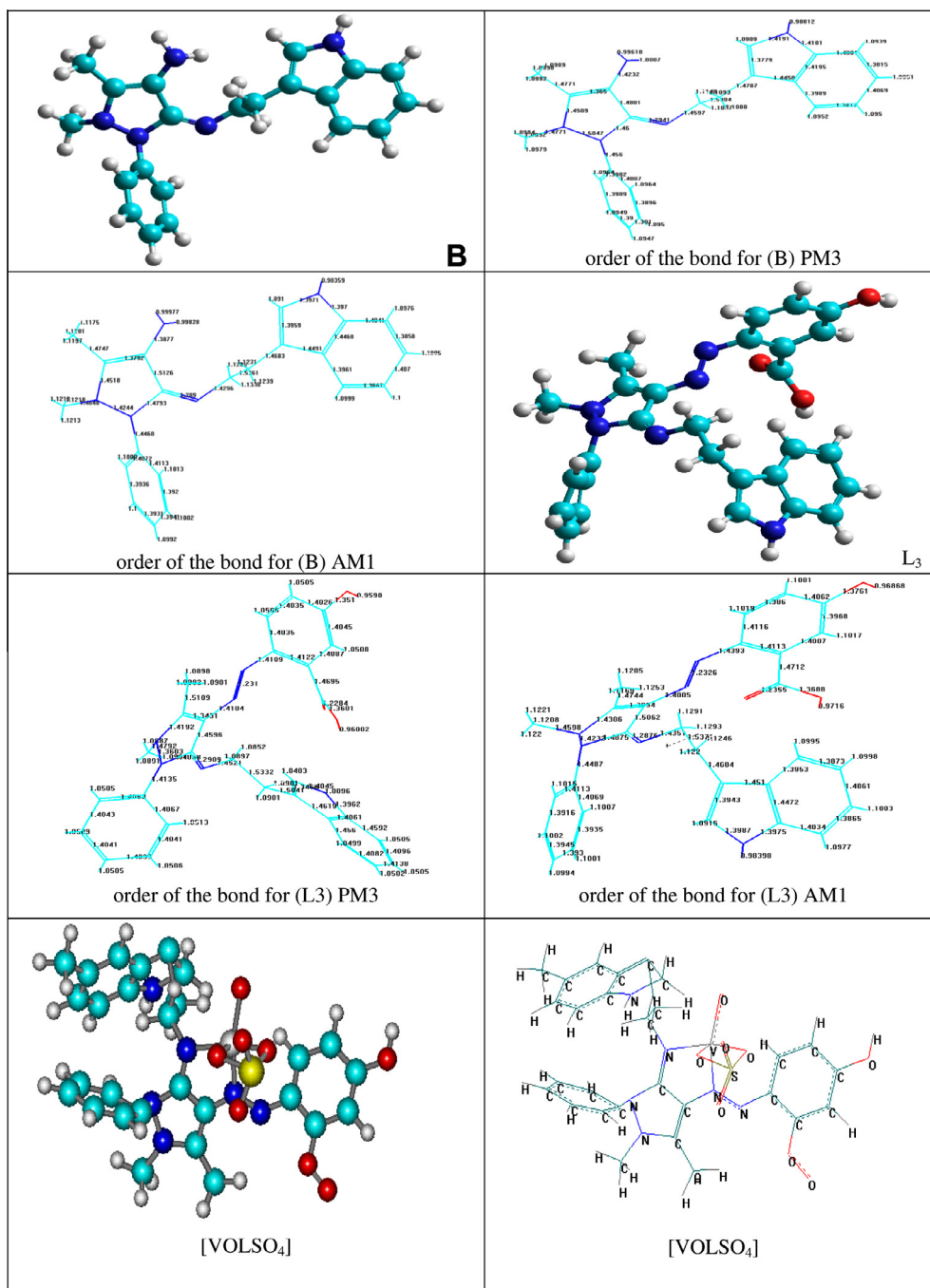
Fig. 1 (*continued*)

3.3. IR spectra

The IR spectra of the compounds A and B show ν(NH) band at 3271 and 3213 cm^{-1}, respectively. Thus, the compounds show absorption bands at 1641 and 1662 cm^{-1} which were attributed to ν(C=O) and ν(C=N), respectively. The spectra of the Azo-schiff base ligands L$_1$ and L$_2$ exhibited bands at 3699, 3429, 3234, 1728, 1601, 1444, 1342 and 1288 cm^{-1} which were attributed to ν(OH) carboxylic, ν(OH) phenolic, ν(NH), ν(C=N), ν(COO) assymmetrical, ν(N=N), ν(COO) symmetrical and ν(CO) phenolic, respectively (Abbas, 2005; Silverstein et al., 1981; Ravichandran and Thangaraja, 2004). On complex formation bands of ν(C=N), ν(N=N) and ν(COO) asymmetry are shifted to the lowering frequencies by (12–22), (10–6) and (19–5) cm^{-1}, respectively, these shifts confirm the coordination of the ligands through the nitrogen of azomethine and the azo groups with metal ion. Moreover, the spectra of the complexes exhibited weak bands between (437–443) and (537–550) cm^{-1} which were attributed to ν(M–O) and ν(M–N), respectively (Nakamoto, 1997). All the characteristic vibrations and assignments of the free ligands and their complexes are listed in Table 2.
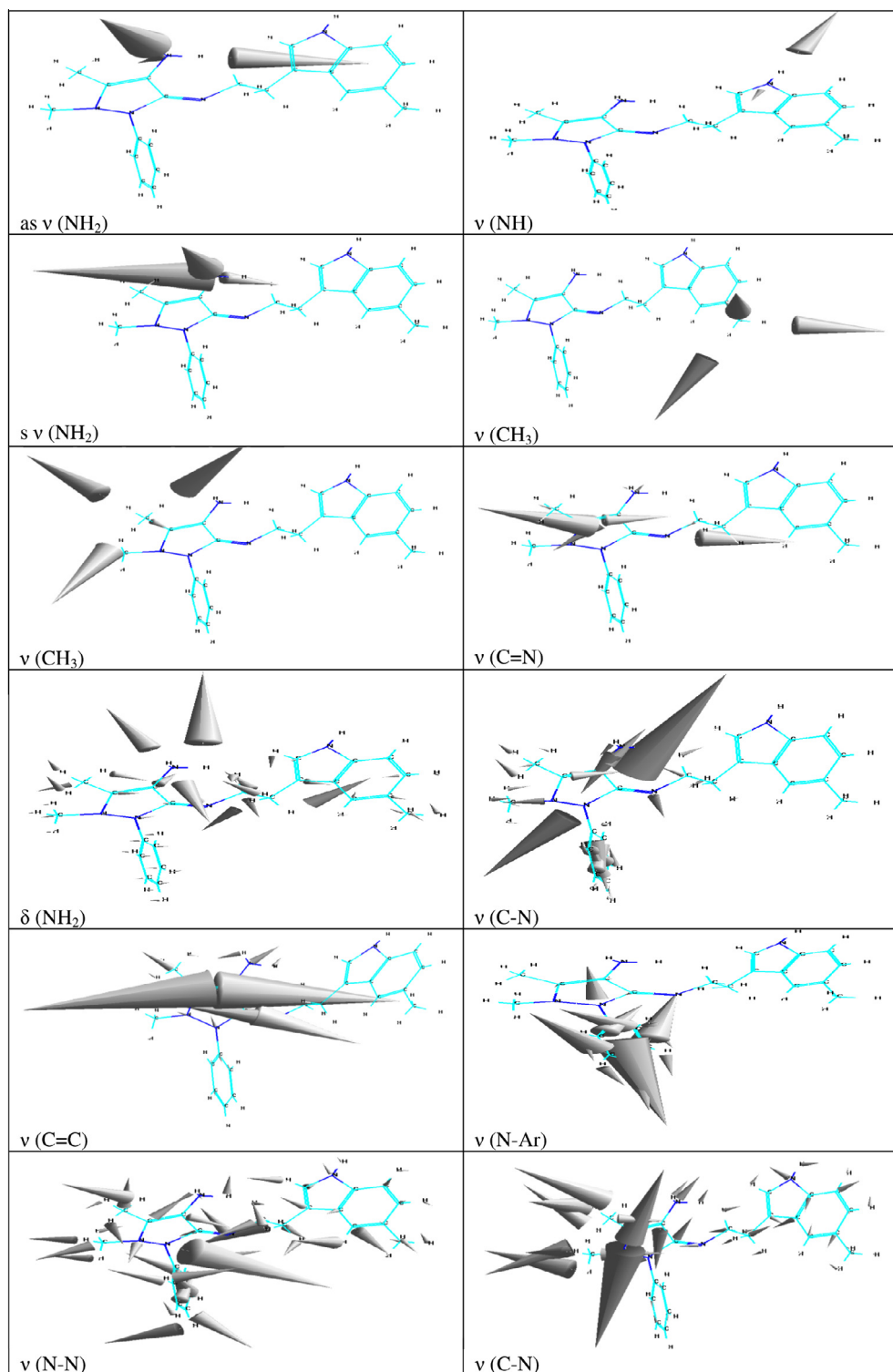
Figure 2 The calculated vibrational frequencies of starting material A (a) and ligand L₁ (b).

3.4. Mass spectrum

3.4.1. Compound (A)

The electron impact spectrum of compound (A) confirms the probable formula by showing a peak at 360 m/z, corresponding to Schiff base moiety [($C_{22}H_{25}N_5$), calculated atomic mass 360]. The series of peaks at 164 m/z is attributed to

($C_{11}H_{18}N$)$^+$ and at 201 m/z attributed to ($C_{11}H_{13}N_4$). Their intensity gives an idea of the stability of fragments.

3.4.2. Compound (B)

The electron impact spectrum of compound (B) confirms the probable formula by showing a peak at (345 m/z), corresponding to Schiff base moiety [($C_{21}H_{23}N_5$), calculated atomic mass

ν (O-H)   ν (O-H)

ν (N-H)   ν (C-O)

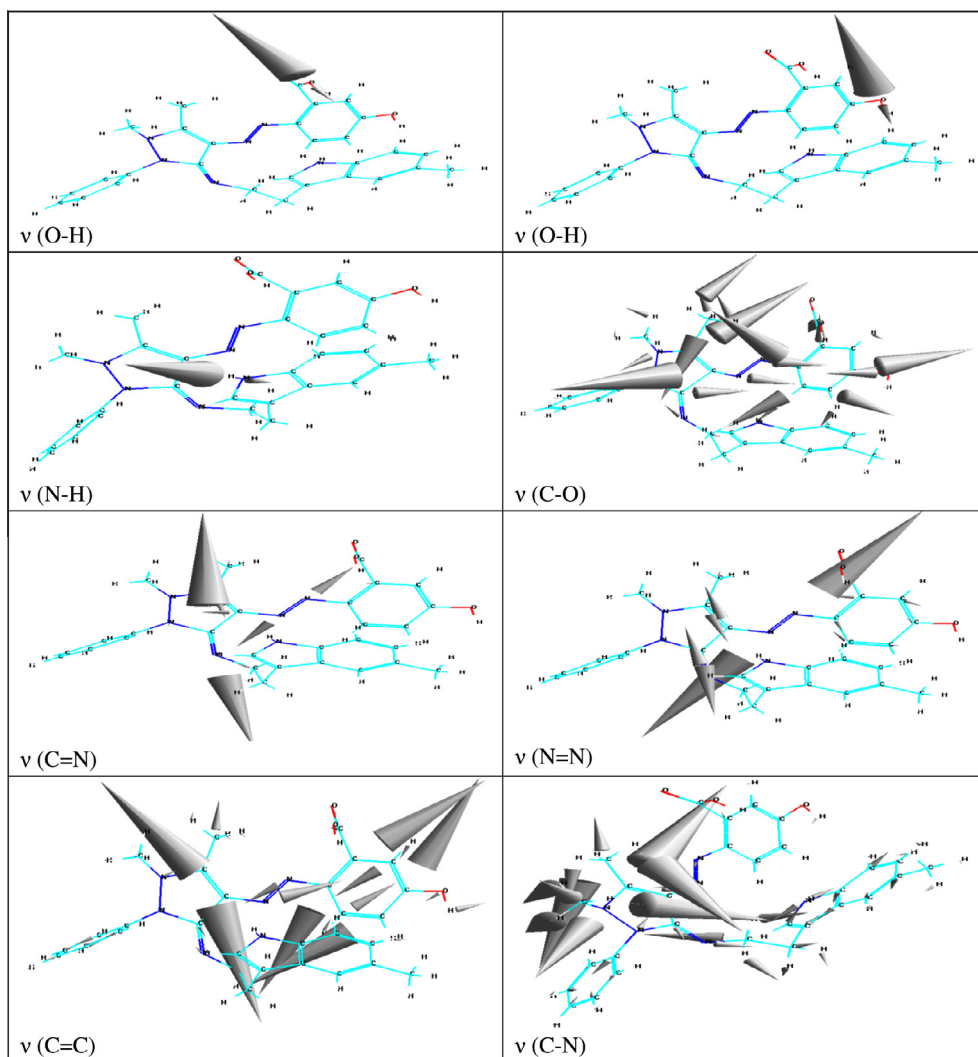ν (C=N)   ν (N=N)

ν (C=C)   ν (C-N)

Fig. 2   (*continued*)

345]. The series of peaks at 201 m/z is attributed to $(C_{11}H_{13}N_4^-)$ and 144 m/z attributed to $(C_5H_9N_4)$. Their intensity gives an idea of the stability of fragments.

3.4.3. Ligand (L$_1$)

The electron impact spectrum of the ligand (L) confirms the probable formula by showing a peak at 508 m/z, corresponding to Schiff base-Azo moiety $[(C_{29}H_{28}N_6O_3)$, calculated atomic mass 508]. The series of peaks in the range of 345 and 159 m/z may be assigned to various fragments. Their intensity gives an idea of the stability of fragments.

3.4.4. Ligand (L$_2$)

The electron impact spectrum of the ligand (L) confirms the probable formula by showing a peak at 494 m/z, corresponding to Schiff base-Azo moiety $[(C_{28}H_{26}N_6O_3)$, calculated atomic mass 494]. The series of peaks in the range of 463,435, 422, 378, 360, 346,328, 252, 241, 226, 213, 189, 174, 148 and 78 m/z

may be assigned to various fragments. Their intensity gives an idea of the stability of fragments.

3.4.5. Complex of VOL$_1$

The electron impact spectrum of [VOL$_1$SO$_4$] confirms the probable formula by showing a peak at 671 m/z, corresponding to Complex moiety $[(C_{29}H_{28}N_6SVO_8)$, calculated atomic mass 671]. The series of peaks in the range of 647, 369, 354, 316, 296, 285, 261, 241, 208, 149 and 101 m/z may be assigned to various fragments. Their intensity gives an idea of the stability of fragments which is attributed to 51 m/z V.

3.4.6. Complex of VOL$_2$

The electron impact spectrum of [VOL$_2$ SO$_4$] confirms the probable formula by showing a peak at 657.5 m/z, corresponding to Complex moiety $[(C_{28}H_{26}N_6VSO_8)$, calculated atomic mass 657.5]. The series of peaks in the range of 430, 429, 227, 205, and 204 m/z may be assigned to various fragments. Their
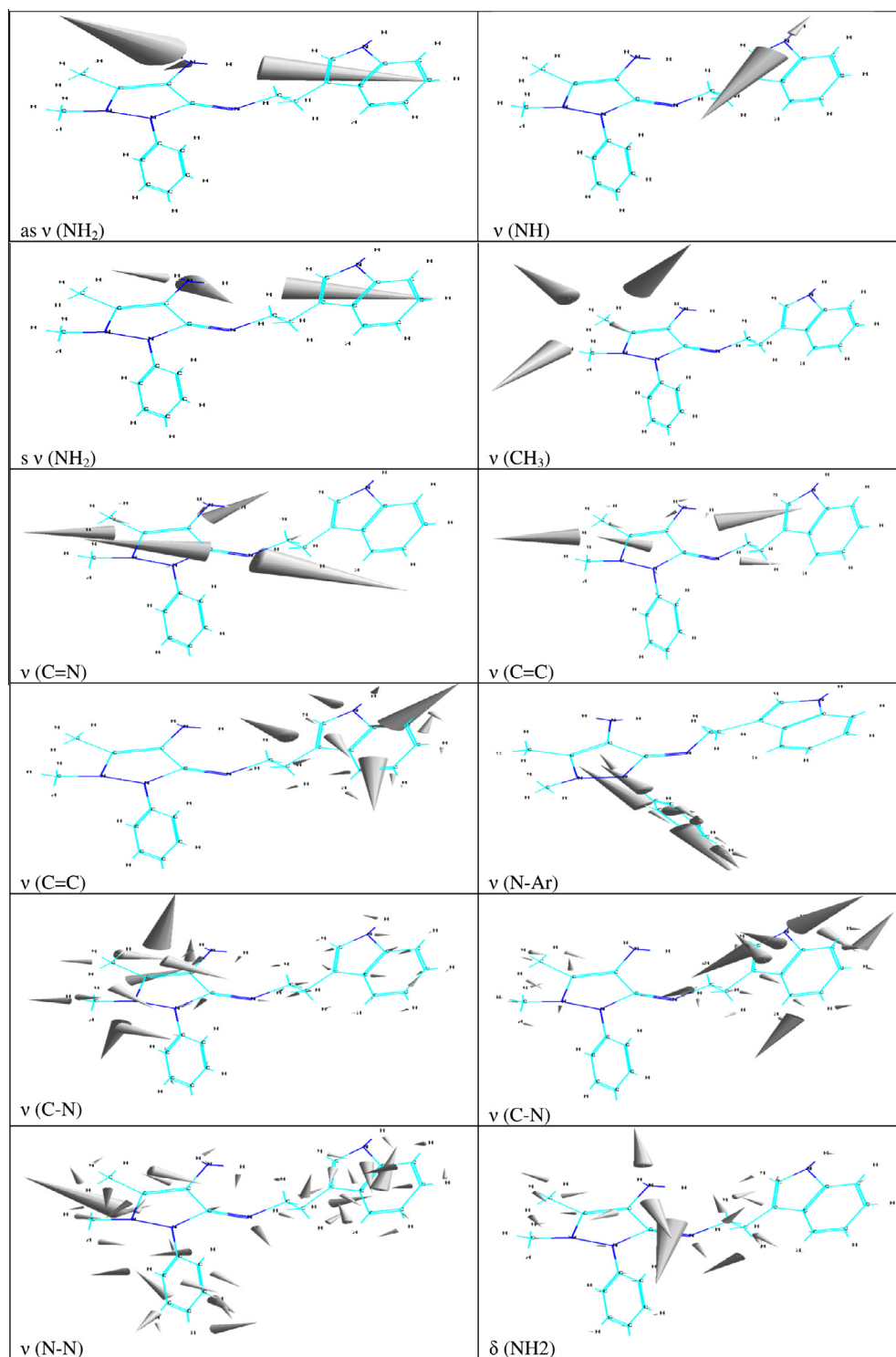
Figure 3 The calculated vibrational frequencies of starting material B (a) and ligand L_2 (b).

intensity gives an idea of stability of fragments which is attributed to 66.4 m/z VO.

3.5. ^1H NMR spectral studies

The newly synthesized ligands gave a satisfactory spectral data and the molecular structure was assigned on the basis of ^1H NMR chemical shift. The identification was based on using simple splitting patterns that were produced by the coupling of protons which have very different chemical shifts. ^1H NMR spectrum of starting material (A) in DMSO-d_6 gives the following signals: phenyl as multiple at 7.64–8.08 ppm, $=$C–CH$_3$ at 1.89 ppm, –C–CH$_3$ at 2.10 ppm, –C–CH$_3$ at 2.74 ppm, –N–CH$_2$ at 2.31 ppm, –N–CH$_3$ at 3.44 ppm, peak

ν (O-H)

ν (O-H)

ν (N-H)

ν (C=N)

ν (N=N)

ν (C-O-H)
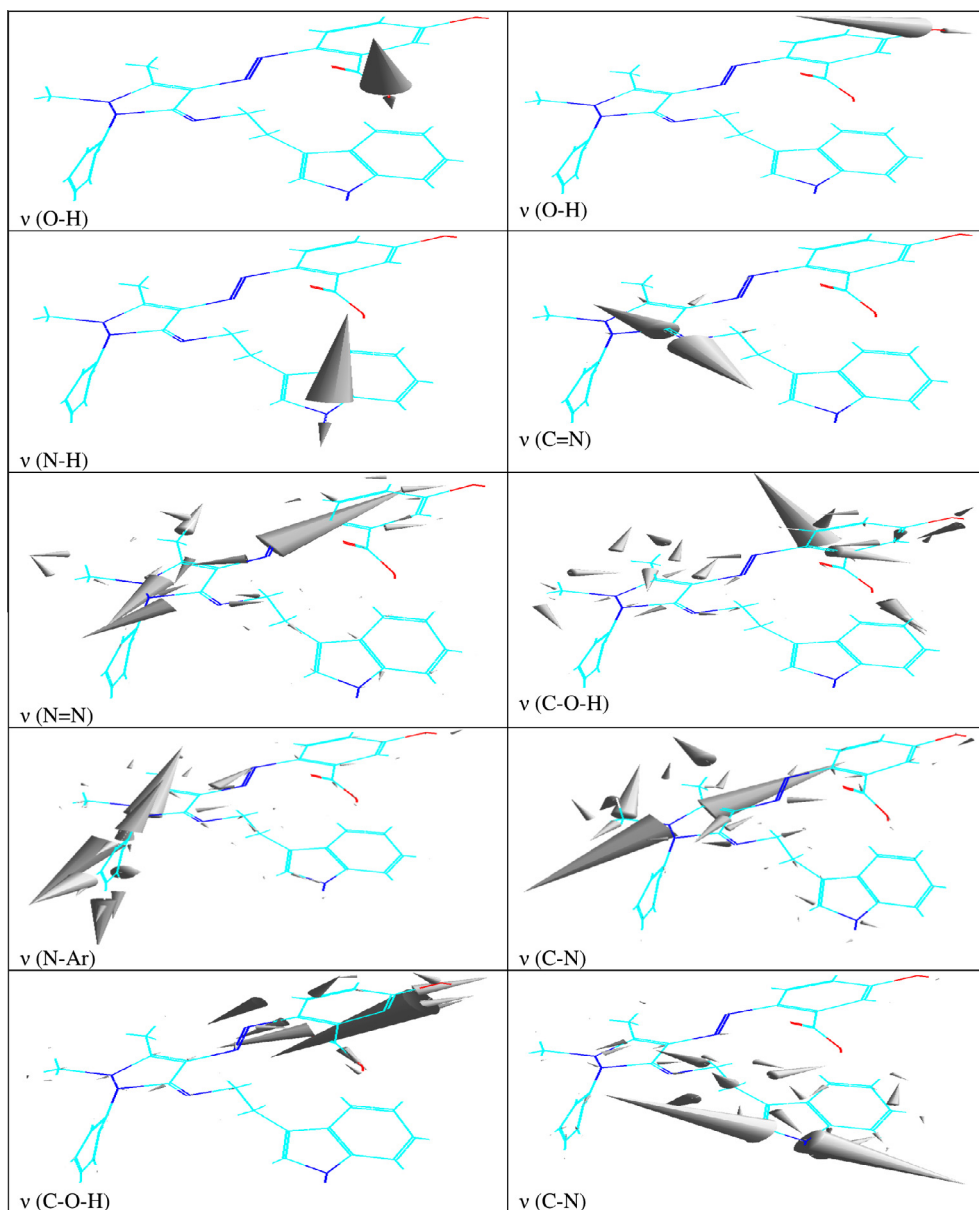
ν (N-Ar)

ν (C-N)

ν (C-O-H)

ν (C-N)

Fig. 3 (continued)

at 12.1 ppm is attributable to the primary amine –NH group, peak at 4.1 ppm is attributable to the amine –NH$_2$ group present in 4-aminoantipyrine of the starting material (A). Moreover, compound (B) in DMSO-d_6 gives the following signals: phenyl as multiple at 7.64–8.08 ppm, $=$C–CH$_3$ at 1.7 ppm, –C–CH$_3$ at 2.74 ppm, –N–CH$_2$ at 2.17 ppm, –N–CH$_3$ at 2.99 ppm, peak at 10.99 ppm is attributable to the primary amine –NH group, peak at 5.99 ppm is attributable to the amine –NH$_2$ group present in 4-aminoantipyrine of the starting material (B) (Sonmez and Sekerc, 2002).

^{1}H NMR spectrum of ligand (L$_2$) in DMSO gives the following signals: phenyl as multiple at 7.00–8.2 ppm, $=$C–CH$_3$ at 1.70 ppm, –N–CH$_2$ at 3.30 ppm, –N–CH$_3$ at 2.10 ppm, peak at 10.99 ppm is attributable to the primary amine –NH group present in the free ligand (L$_2$)., peaks at 4.49 and 12.11 ppm are attributable to the phenolic –OH group and carboxylic-OH group, respectively, of the free ligand. The (L$_1$) in DMSO

gives the following signals: phenyl as multiple at 7.00–8.2 ppm, $=$C–CH$_3$ at 1.89 ppm, –C–CH$_3$ at 2.10 ppm, –C–CH$_3$ at 2.74 ppm, –N–CH$_2$ at 3.01 ppm, –N–CH$_3$ at 3.44 ppm, peak at 12.11 ppm is attributable to the primary amine –NH group present in the free ligand (L)., peaks at 4.49 and 13.0 ppm are attributable to the phenolic –OH group and carboxylic-OH group, respectively, of the free ligand (Abbas and Shayma, 2011).

3.6. Thermal analyses TGA

The results of thermo gravimetric analyses of L$_1$, L$_2$ and VO(II) complexes are given in Table 3. The thermograms have been carried out in the range of 25–700 °C at a heating rate of 10 °C/min in nitrogen atmosphere, they showed an agreement in weight loss between their results obtained from the thermal

Table 6 Comparison of experimental and theoretical vibration frequencies for ligands.

Compound	asv(NH$_2$)	(NH$_2$)vs	v(C=N)	v(C–N)	v(N=N)	v(C=C)	v(NH)	δ(NH$_2$)	v(OH) phenol	v(OH) carboxylic	v(C–O) phenol
A	3485* 3504** 0***	3305* 3382** * 0***	1641 1633* 1867** −0.001*** *	1243* 1249** 0***		1591–1556* 1832** −0.001***	3271* 3452** 0***	1612* 1021** 0.003***			
L$_1$	– –	– –	1728* 1891** 0***	1276* 1341** 0***	1072* 1874** −0.007***	1589–1554* 1779** −0.001***	3234* 3456** 0***	–	3699* 3890** 0***	3429* 3885* −0.001***	1288* 1412** 0***
B	3433* 3505* 0***	3329* 3383* * 0***	1662 −1635** 1866** −0.001**	1230* 1249** 0***	–	1589–1496* 1832** −0.001***	3213* 3454** 0***	1608* 1023* 0.003***	– –		
L$_2$	– –	– –	1738* 1899** 0***	1276* 1377** 0***	1056* 1473** −0.003***	1589–1554* 1476** 0***	3234* 3571** 0.001** *	–	3692* 3980** 0***	3429* 3812* −0.001***	1288* 1350** 0***

* Experimental frequency.

** Theoretical frequency.

*** Error% due to main difference in the experimental measurements and theoretical treatments of vibration spectrum.

decomposition and the calculated values, which supports the results of elemental analysis and confirms the suggested formulae. Thus, the ligand L$_1$ showed a common general behavior as the first step (C$_{23}$H$_{23}$N$_5$O$_3$) was loss of C$_6$H$_5$N moiety followed by the other parts of the ligand L$_1$. Moreover, the ligand L$_2$ decomposed in the first step (C$_{21}$H$_{20}$N$_4$O) which was loss of C$_7$H$_6$N$_2$O$_2$ moiety followed by the other parts of the ligand L$_2$. Furthermore, the final step of the thermolysis reactions of the complexes was found to give the metal oxide (L$_1$) = C$_{29}$H$_{28}$N$_6$O$_3$ [101.131% Found (99.999% Cal) (158–348 °C) → C$_{23}$H$_{23}$N$_5$O$_3$ [82.648% Found (82.085% Cal)] (348–598 °C) → C$_6$H$_5$N$^-$ [18.483% Found (17.914%Cal).

(L$_2$) C$_{28}$H$_{26}$N$_6$O$_3$ [102.231% Found (99.999% Cal)] (153–355 °C) → C$_{21}$H$_{20}$N$_4$O [70.890% Found (69.642% Cal)] (355–596 °C) → C$_7$H$_6$N$_2$O$_2$ [31.341% Found (30.357% Cal)].

1-C$_{29}$H$_{28}$N$_6$O$_8$SV (671.58) (30–415 °C) → C$_{17}$H$_{17}$NO$_3$ [42.814% Found (42.22% Cal)].

2-C$_{12}$H$_{11}$N$_5$O$_5$SV (283) (415–600 °C) → C$_{12}$H$_{17}$N$_5$O$_4$S [48.578% Found (48.786% Cal)].

3-VO [8.608% Found (9.976% Cal)].

Total wt. loss = 91.392% Found (91.006% Cal) and final residue: 8.608% Found (8.994% Cal).

1-C$_{29}$H$_{28}$N$_6$O$_8$SV (657.55) (30–410 °C) → C$_{17}$H$_{17}$NO$_3$ [42.814% Found (42.22% Cal)].

2-C$_{12}$H$_{11}$N$_5$O$_5$SV (393.05) (410–600 °C) → C$_{12}$H$_{17}$N$_5$O$_2$ [40.786% Found (40.225% Cal)].

3-VO$_3$S [16.4% Found (17.555% Cal)].

Total wt. loss = 83.6% Found (82.445% Cal) and final residue: 6.4% Found (15.055% Cal).

3.7. Kinetic studies

Coats–Redfern is the method mentioned in the literature related to decomposition kinetics studies; this method is applied in this study (Coats and Redfern, 1964). From the TG curves, the activation energy, E, pre-exponential factor, A, entropy,

ΔS, enthalpy, ΔH, and Gibbs free energy, ΔG were calculated by the Coats–Redfern method where: ΔH = E − RT and ΔG = ΔH − TΔS.

Kinetic parameters are calculated by employing the Coats–Redfern equations, are summarized in Table 4. The Coats–Redfern equation may be written as the following:

$$log\left[\frac{1-(1-\alpha)^{1-n}}{T^2(1-n)}\right] = log\frac{ZR}{qE}\left[1-\frac{2RT}{E}\right]$$
$$-\frac{E}{2.303RT}\quad n\neq1 \text{ for complex} \qquad (1)$$

$$log\left[\frac{-log(1-\alpha)}{T^2}\right] = log\left[\frac{AR}{\beta E}\left(1-\frac{2RT}{E}\right)\right]\frac{E}{2.303RT}$$
$$n\neq1 \text{ for ligands} \qquad (2)$$

where α is the mass loss at the completion of the reaction, R is the gas constant, Ea is the activation energy in J mol^{-1} and q is the heating rate. Since 1–2 RT/Ea≈ = 1, a plot of the left-hand side of the above equation against and ΔE* was calculated from the slope and A (Arrhenius constant) was found from the intercept. The activation entropy ΔS*, the activation enthalpy ΔH* and the free energy of activation ΔG* were calculated using the following equations:

$$S^* = 2:303(logAh/KT)R; H^* = E^* - RT; G^*$$
$$= H^* - T_SS^*\cdots3 \qquad (3)$$

where K and h are the Boltzmann's and Planck's constants, respectively. The calculated values of ΔE*, ΔS*, ΔH* and ΔG* for the dehydration and the decomposition steps are given in Table 4. The activation energies of the decomposition were found to be in the range of 134–208 J mol^{-1}.According to the kinetic data obtained from TGA curves, the negative values of activation entropies ΔS* indicate more ordered activated complexes than the reactants and the reaction is slow (Frost and Pearson, 1961).
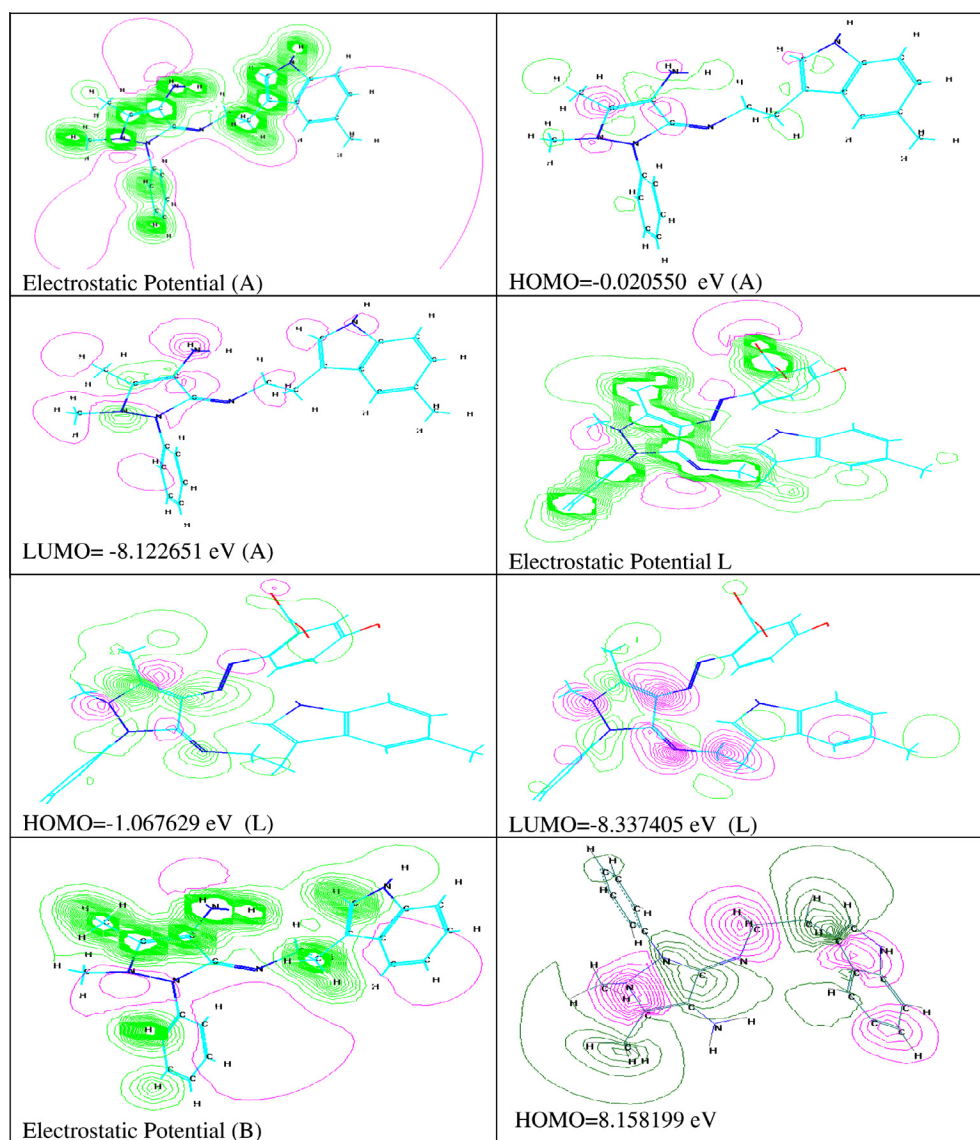
Figure 4 HOMO and electrostatic potential for starting material and L.

3.8. Theoretical study

The vibration spectra of A, B and Azo-schiff base (L₁ and L₂) were calculated by using a semi-empirical (PM3 and AM1) method. The results obtained for wave numbers are presented in (Table 5), and the comparison with the experimental values indicate some deviations. These deviations may be due to the harmonic oscillator approximation and lack of electron correlation. It was reported (Chamberlain et al., 1999) that frequencies coupled with Hartree- Fock Theory (HFT) approximation and quantum harmonic oscillator approximation tend to be 10% too high.

3.8.1. Optimized geometries' energy of metal complexes for Schiff base-Azo

Theoretical probable structures of metal complexes with Azo-Schiff base were calculated to search for the most probable model building stable structure, these shapes, show the calculated optima geometries for A, B and Azo-Schiff base (L₁

and L₂) and their vanadyl complexes as shown in (Figs. 1–3). The results of PM3 method of calculation in the gas phase for binding energies and heat of formation of complexes are described in Table 5. The comparison of experimental and theoretical vibration frequencies is tabulated in Table 6.

3.8.2. Electrostatic potential (E.P)

Electron distribution governs the electrostatic potential of molecules and describes the interaction of energy of the molecular system with a positive point charge, so it is useful to find sites of reaction in a molecular positive charged species that tend to attack a molecule where the E.P. is strongly negative electrophilic attach (Druckerey and Mark, 2006).The E.P of free ligands was calculated and plotted as 3D contour to investigate the reactive sites of the molecules, and one can interpret the stereochemistry and rates of many reactive involving soft electrophiles and nucleophiles in terms of the properties of frontier orbitals (HOMO and LUMO). Overlap between the HOMO and LUMO values was plotted as 3D contour to get more information about these molecules. The results of calcu-
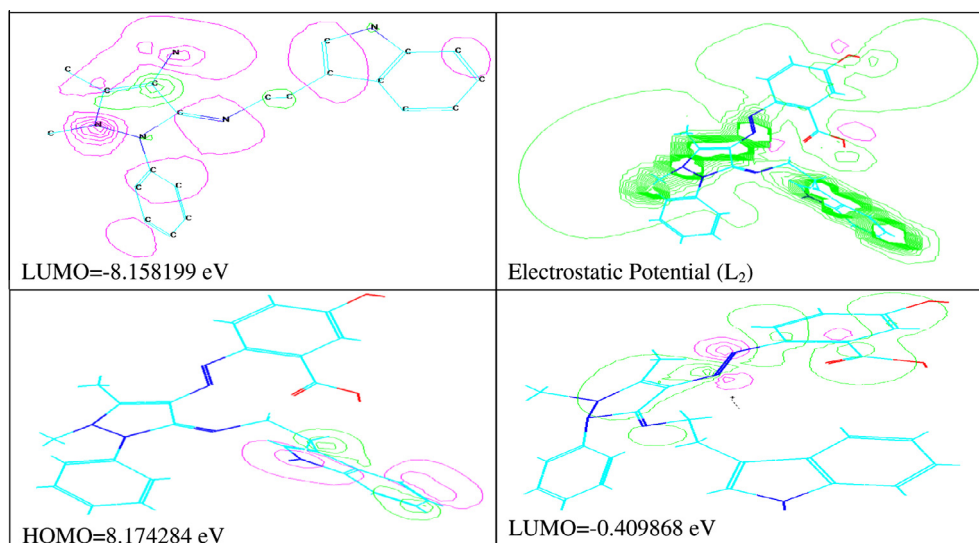
| LUMO=-8.158199 eV | Electrostatic Potential (L$_2$) |
| HOMO=8.174284 eV | LUMO=-0.409868 eV |

Fig. 4   (*continued*)

Table 7 Antibacterial activity data of ligands and their complexes as inhibition zone (mm).

Compound	*Bacillus subtilis* G$^+$	*Staphylococcus aureus* G$^+$	*Escherichia coli* G$^-$	*Pseudomonas aeruginosa* G$^-$
L$_1$	20	17	19	16
L$_2$	22	20	22	18
[VOL$_1$SO$_4$]	24	22	24	22
[VOL$_2$SO$_4$]	20	20	16	21

Key to interpretation: Less than 10 mm = inactive, 10–15 mm = weakly active, 15–20 mm = moderately active, more than 20 mm = highly active.

lation showed that the LUMO of transition metal ion prefers to react with the HOMO of nitrogen atoms of Azo- Schiff base ligands as shown in (Fig. 4).

3.9. Microbiological investigation

The biological activity of L$_1$ and L$_2$ ligands and their vanadyl complexes was tested against bacteria; we used more than one test organism to increase the chance of detecting antibiotic principles in tested materials. The organisms used in the present investigation included two Gram positive bacteria (*B. subtilis* and *S. aureus*) and two Gram negative bacteria (*E. coli* and *P. aeruginosa*). The results of the bactericidal screening of the synthesized compounds are recorded in Table 7. An influence of the central ion of the complexes in the antibacterial activity against the tested Gram positive and Gram negative organisms shows that the complexes have an enhanced activity compared to the ligands itself.

4. Conclusion

In this paper, the synthesis and coordination chemistry of some monomeric complexes obtained from the reaction of the ligands L$_1$ and L$_2$ with some VO(VI) were explored. The mode of bonding and overall structure of the complexes were determined through physico-chemical and spectroscopic methods. Complex formation study via molar ratio was investigated and results were consistent to those found in the solid complexes with a ratio of (M:L) as (1:1). The thermodynamic parameters, such as ΔE^*, ΔH^*, ΔS^* ΔG^* and K are calculated from the TGA curve using the Coats-Red fern method. Hyper Chem-6 program was used to predict structural geometries of compounds in gas phase. The heat of formation (ΔH_f°) and binding energy (ΔE_b) at 298 K for the free ligands and their vanadyl complexes were calculated by PM3 method. The synthesized ligands and their metal complexes were screened for their biological activity against bacterial species, two Gram positive bacteria (*B. subtilis* and *S. aureus*) and two Gram negative bacteria (*E. coli* and *P. aereuginosa*).

References

Abbas, A.S., Shayma, A.S., 2011. J. Orient. Chem. 27, 835–845.

Abbas, A.S., 2005. J. Um-Salama Sci. 2, 395–602.

Aiello, I., Ghedini, M., Neve, F., Pucci, D., 1997. Chem. Mater. 9, 2107.

Bernal, I., 1990. Stereochemical Control, Bonding and Steric Rearrangements. Elsevier, Amsterdam (Chapter 3).

Bryliakov, K.P., Talsi, E.P., 2004. Angew. Chem., Int. Ed. 43, 5282.

Cambel, E.J., Nguyen, S.T., 2001. Tetrahedron Lett. 42, 1221.

Chamberlain, B.M., Sun, Y., Hagadorn, J.R., Hemmesch, E.W., Hillmyer, A.V., Tolman, W.B., 1999. Macromolecules 32, 2400.

Coats, A.W., Redfern, J.P., 1964. Nature 68, 201.

Dorestt, H.A., 1996. A review of quantum chemical studies of energetic materials, DSTO Technical report.

Druckerey, H., Mark, H.F., 2006. Benzene Diazonium Salts-Azo Dyes 1, 123.

Dyers, J.L., Que, S.Y., Van Derveer, D., Bu, X.R., 2006. Inorg. Chim. Acta 359, 197.

El Halabieh, R.H., Mermut, O., Christopher, B., 2004. J. Pure Appl. Chem. 76, 1445.

Foresman, J.C., Frisch, C., 1996. Exploring Chemistry with Electronic Structure Methods, second ed. Gaussian Inc., Springer, Berlin.

Frost, A.A., Pearson, R.G., 1961. Kinetics and Mechanism. Wiley, New York.

Golcu, A., Tumer, M., Demirelli, H., Wheatley, R.A., 2005. Inorg. Chim. Acta, 358.

Gupta, R., Saxena, R.K., Chatarvedi, P., Virdi, J.S., 1995. J. Appl. Bacteriol. 78, 378.

Klement, R., Stock, F., Elias, H., Paulus, H., Valko, M., Mazur, M., 1999. Polyhedron 18, 3617.

Lever, A.B.P., 1968a. Inorganic Electronic Spectroscopy. Elsevier, New York, NY, USA.

Lever, A.B.P., 1968b. Mol. Catal. A: Chem. 160, 217.

Nakamoto, K., 1997. Infrared and Raman Spectra of Inorganic and Coordination Compounds. Wiley-Inter Science, New York.

Nishihara, H., 2004. Bull. Chem. Soc. Jpn. 77, 407.

Pui, A., Pierre, M.J., 2007. Polyhedron 26, 3143–3152.

Ravichandran, N.S., Thangaraja, C., 2004. J. Chem. Sci. 116, 215–219.

Santos, I.C., Vilas-Boas, M., Piedade, M.F.M., Freire, C., Durate, M.T., Castro, B., 2000. Polyhedron 19, 655.

Shayma, A.S., Yang, F., Sadia, M., Mohean, E., 2010. Sains Malaysiana 39, 957–962.

Silverstein, R.M., Bassler, G.C., Movril, T.C., 1981. Spectroscopic Identification of Organic Compounds, fourth ed. Wiley, New York.

Sonmez, M., Sekerc, M., 2002. Pol. J. Chem. 76, 907–914.

Stemmler, A.J., Burrows, C.T., 1999. J. Am. Chem. Soc. 121, 6956.

Ueno, T., Yokoi, N., Unno, M., Matsui, T., Tokita, Y., Yamada, M., Ikeda, S.M., Nakajima, H., Watanabe, Y., 2006. PNAS 103, 9416.

Vigato, P.A., Tamburini, S., 2004. Coord. Chem. Rev. 248, 1717.